A Sparse Image Method for BEM Capacitance Extraction*

Byron Krauter
IBM Corp.
11400 Burnet Road
Austin, TX 78758
krauter@austin.ibm.com

Yu Xia
AMD Corp.
5900 E. Ben White Blvd
Austin, TX 78741
yxia@beast.amd.com

Aykut Dengi
SEMATECH Inc.
2706 Montopolis Drive
Austin, TX 78741
Aykut.Dengi@sematech.org

Lawrence T. Pileggi
Electrical and Computer Engineering
Carnegie Mellon University
Pittsburgh, PA 15213
pileggi@ece.cmu.edu

Abstract—Boundary element methods (BEM) are often used for complex 3-D capacitance extraction because of their efficiency, ease of data preparation, and automatic handling of open regions. BEM capacitance extraction, however, yields a dense set of linear equations that makes solving via direct matrix methods such as Gaussian elimination prohibitive for large problem sizes. Although iterative, multipole-accelerated techniques have produced dramatic improvements in BEM capacitance extraction, accurate sparse approximations of the electrostatic potential matrix are still desirable for the following reasons. First, the corresponding capacitance models are sufficient for a large number of analysis and design applications. Moreover, even when the utmost accuracy is required, sparse approximations can be used to precondition iterative solution methods.

In this paper, we propose a definition of electrostatic potential that can be used to formulate sparse approximations of the electrostatic potential matrix in both uniform and multilayered planar dielectrics. Any degree of sparsity can be obtained, and unlike conventional techniques which discard the smallest matrix terms, these approximations are provably positive definite for the troublesome cases with a uniform dielectric and without a groundplane.

I. Introduction

Decreasing feature sizes and increasing die sizes in high performance VLSI design have combined to make interconnect delay a critical factor in determining final circuit speeds [14]. Therefore, 3-D capacitance extraction on interconnect wiring has become increasingly important. While post-layout extraction is necessarily rule-based to improve efficiency (analytical or table-look-up models derived from complex 3-D analyses [3] are selectively applied during run time according to shapes recognition algorithms), shapes are commonly encountered for which rules are not available. Because complex 3-D modeling of these shapes is too costly, an approximate 3-D model is warranted. This paper takes a step in this direction. A sparse approximation of the potential matrix is formulated, and when this matrix is applied to BEM capacitance extraction, a practical upper bound on the total capacitance for each conductor is obtained.

II. Background

The following paragraphs briefly describe conventional BEM capacitance extraction for a system of K conductors in a homogenous or uniform dielectric. Although non-uniform dielectrics can also be analyzed using boundary element methods (semi-infinite interfaces are handled with a different Green's function [13]), these complications are omitted here for reasons of clarity.

Because the solution to Possion's equation in a homogeneous dielectric is uniquely specified by the boundary conditions [5], BEM capacitance extraction begins with a discretization of the conductor surfaces, and an evaluation of the surface potentials as functions of the surface charge densities. That is, each of the K conductor surfaces is divided into a set of N_k contiguous panels, and the surface potential at a point r_i on conductor i is

$$\Phi_i(r_i) = \sum_{k=1}^{K} \left[\sum_{n=1}^{N_k} \int_{S_n} G(r_i, r)\, \sigma_n(r)\, dS_n \right] \quad (1)$$

where $\sigma_n(r)$ is the charge density on the conductor surface S_n and $G(r_i, r)$ is the Green's function for an infinite dielectric:

$$G(r_i, r) = \frac{1}{4\pi\varepsilon_r\varepsilon_0} \frac{1}{|r_i - r|} \quad (2)$$

The integral equations represented by (1) can be reduced to a matrix equation through a mathematical procedure called the method of moments [4]. (Equivalent to variational formulations, the method of moments procedure is a weighted residual technique [2], and as such, minimizes the error that is inherent with the discretization of such problems). The surface charge density $\sigma(r)$ on each panel can be removed from the integral sign through the use of the mean value theorem [1]. And if (1) is integrated over cell i, a solution by Galerkin's method results [16]:

$$\Phi_i = \sum_{k=1}^{K} \sum_{n=1}^{N_k} \frac{q_n}{S_i S_n} \int_{S_i} \int_{S_n} G(r_i, r)\, dS_i\, dS_n \quad (3)$$

The problem can now be cast into the matrix equation

$$[\Phi] = [P][Q] \quad (4)$$

where $[\Phi] = [\Phi_1\ \Phi_2\ \cdots\ \Phi_n]^T$ and $[Q] = [Q_1\ Q_2\ \cdots\ Q_n]^T$ represent the discrete panel potentials and panel charges respectively, and $[P]$ is the potential or influence matrix between these cells. The coefficients of $[P]$ are

$$p_{ij} = \frac{1}{S_i S_j} \int_{S_i} \int_{S_j} G(r_i, r)\, dS_j\, dS_i \quad (5)$$

* This work was supported in part by the Semiconductor Research Corporation under contract 95-DC-068 and International Business Machines.

33rd Design Automation Conference ®

DAC 96 - 06/96 Las Vegas, NV, USA

The short circuit capacitance matrix, C_{ss}, can be obtained from the inverse of the potential matrix, P^{-1}, and an incidence matrix A that relates the discrete surface cells to the K conductors. That is, A_{ij} is 1 if cell *i* resides on conductor *j* and is 0 otherwise. In matrix algebra, C_{ss} is given by

$$\left[C_{ss}\right] = \left[A\right]^{T}\left[P\right]^{-1}\left[A\right] \tag{6}$$

While (6) is certainly concise, it is not particularly enlightening for most readers. Therefore, the derivation of C_{ss} is generally described in a more piecemeal fashion.

For example, to determine C_{ij}, we first solve for the panel or cell charges that result when a one volt potential is applied to the j*th* conductor relative to all other conductors. That is, we solve the simultaneous linear equations:

$$\left[P\right]\left[q\right] = \begin{bmatrix} 0 \\ 0 \\ \vdots \\ 1 \\ 1 \\ \vdots \\ 0 \\ 0 \end{bmatrix} \begin{matrix} \\ \\ \\ \text{1 Volt Applied} \\ \text{to j}th\text{ conductor} \\ \\ \\ \\ \end{matrix} \tag{7}$$

Then to determine the individual matrix term C_{ij}, we sum all of the panel charges on the i*th* conductor.

The resulting C_{ss} matrix is symmetric and diagonally-dominant. The off-diagonal terms of the C_{ss} matrix are negative and equal in magnitude to the total capacitive coupling between the two conductors represented by that row and column number. The diagonal terms are positive and equal the sum of all capacitances to the conductor given by that row and column number. This total includes the capacitance to the reference node which is often located at infinity:

$$C_{ii} = C_{i \text{ to reference}} + \sum_{i \neq j} (-C_{ij}) \tag{8}$$

If the reference level is located at infinity (since charge cannot be drawn from infinity), the short circuit capacitance matrix is first converted to a two-terminal capacitance matrix, and then the two-terminal capacitance matrix is converted to a node pair capacitance matrix [10]. If a ground plane is present and charge can be drawn from the reference level, the short circuit capacitance matrix directly yields a two-terminal capacitance matrix.

III. Shift &Truncate Electrostatic Scalar Potential

An approximate formulation of magnetic vector potential is described in [9] that yields sparse yet provably positive-definite partial inductance matrices. This formulation no longer assumes that currents are imaged (or return) at infinity. Instead, it assumes all incremental current vectors are imaged (or return) at a finite or constant radius r_o from their origin. In this paper, a similar definition is applied to the electrostatic potentials in both uniform and planar multilayered dielectrics. The new electrostatic potential function for a unit point charge is formulated such that the zero potential lies at a constant radius r_o from the charge. For example, the shift-and-truncate electrostatic potential due to a point charge (at the origin) in an infinite uniform dielectric (with a relative dielectric constant ε_r) is:

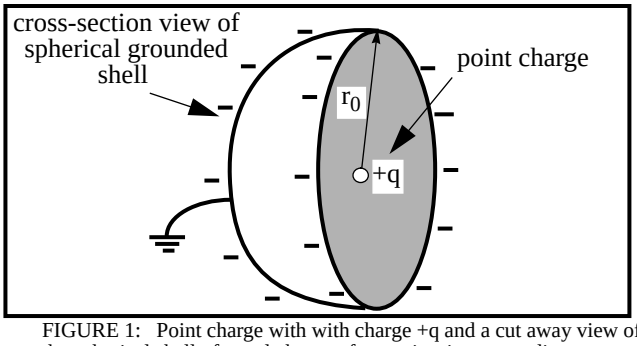

FIGURE 1: Point charge with with charge +q and a cut away view of the spherical shell of equal charge of opposite sign at a radius r_0.

$$\begin{aligned} V(r, r_o) &= \frac{1}{4\pi\varepsilon_r\varepsilon_0}\left(\frac{1}{r} - \frac{1}{r_o}\right), && r_o \geq r \\ &= 0, && r_o < r. \end{aligned} \tag{9}$$

We may visualize this as the effect of an imaginary grounded sphere of radius r_o around each the point charge (see Fig.1).

When a ground plane (the simplest multilayered dielectric) is considered, (10) is simply applied to the electrostatic potentials induced by both the point charge and its image, and a variation to the method of images solution results. If r_{+q} and r_{-q} in Fig.2 are the respective separations between an observation point and a point charge and its image, the shift and truncate potential formulation is

$$\begin{aligned} V\left(r_{+q}, r_o\right) &= \frac{1}{4\pi\varepsilon_r\varepsilon_0}\left(\frac{1}{r_{+q}} - \frac{1}{r_{-q}}\right), && r_{-q} < r_o \\ &= \frac{1}{4\pi\varepsilon_r\varepsilon_0}\left(\frac{1}{r_{+q}} - \frac{1}{r_o}\right), && r_{+q} < r_o < r_{-q} \\ &= 0, && r_o < r_{+q} \end{aligned} \tag{10}$$

When more complex interface boundaries are considered, method of images solutions generally cannot be expressed with a finite set of image charges [17]. Consider the simple double-interface example depicted in Fig.3. A point charge +q is located in the thin dielectric medium ε_1 at a distance (a) from a semi-infinite ground plane below, and at a distance (b) from a semi-infinite dielectric medium ε_2 above. The ground plane and the two dielectric mediums ε_1 and ε_2 are respectively labeled in this figure as Regions 0, 1, and 2, and the magnitude and location of the first order image charges are

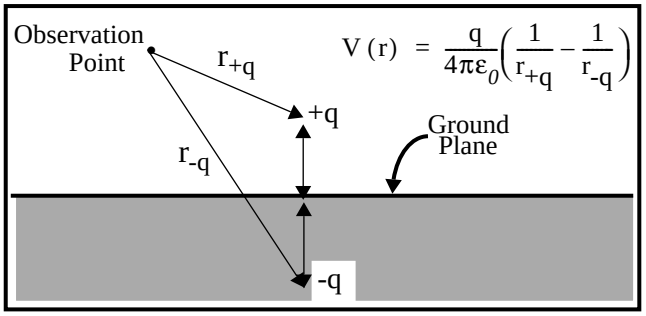

FIGURE 2: Method of image solution for potential due to a point charge above a ground plane.

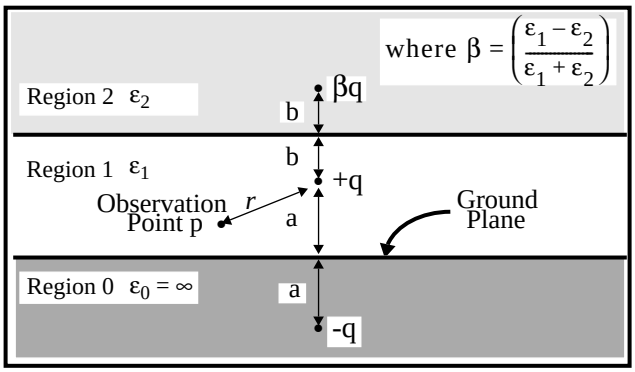

FIGURE 3: First order image charges for a point charge (+q) and observation point inside a thin dielectric medium e1 which is above a ground plane and below a dielectric medium ε2.

shown. (To simplify subsequent equations, the location of the point charge +q is considered to be the origin in Fig.3.)

The electrostatic potential at the observation point p in Region 1 (which is separated by a distance *r* from the point charge +q) can be expressed as a sum of the electrostatic potentials (in an infinite dielectric ε_1) due to the point charge +q at the origin and its image charges both directly above and directly below.

$$V_p(r) = \frac{1}{4\pi\varepsilon_1}\left(\frac{q}{r} + \sum_{i=0}^{\infty}{}^{\text{Reg 0}}\frac{q_i}{|z_i - r|} + \sum_{j=0}^{\infty}{}^{\text{Reg 2}}\frac{q_j}{|z_j - r|}\right) \quad (11)$$

In (12), q_i and q_j represent the magnitude, and z_i, and z_j the locations of image charges in Regions 0 and 2 respectively. The magnitudes and locations of the entire infinite sequence of image charges for Fig.3 are summarized in Fig.4.

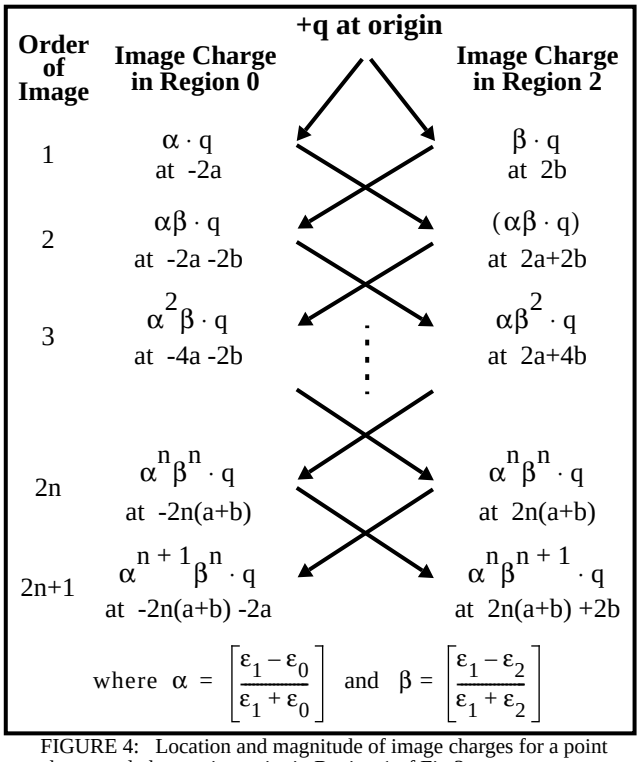

FIGURE 4: Location and magnitude of image charges for a point charge and observation point in Region 1 of Fig.3.

When the shift and truncation formulation is applied to this more complex structure, (10) is simply applied to the electrostatic potentials induced by both the point charge and its images. Because r_0 is finite, the infinite series in (12) truncates when $|z - r| > r_0$.

IV. Stability of Sparse Image Method Approximations

Like the sparse partial inductance matrices presented in [9], the sparse matrix approximations that result from (10) are provably positive-definite for uniform dielectrics. The following paragraphs outline a proof for an infinite, uniform dielectric without a ground plane. The proof for an infinite, uniform dielectric with a ground plane is similar, but is omitted here for the sake of brevity.

The energy, U_E, stored in a static electric field is equal to the assembly energy required to establish that field and is given by

$$U_E = \frac{1}{2}\int \rho V \, d\tau \quad (12)$$

where the volume integral includes all regions in which the charge density, ρ, is non-zero [11]. For a finite system of stationary charges in uniform dielectric, this assembly energy can be related to the volume integral taken over all space, of the electric field squared (E^2), and is therefore, guaranteed to be positive.

$$U_E = \frac{\varepsilon_r \varepsilon_0}{2}\int_{\infty} E^2 dV \geq 0 \quad (13)$$

U_E can also be related to the quadratic form of the potential matrix.

Consider a system of conductors where each conductor surface has been divided into contiguous panels and the total number of panels is N. The volume integral of ρV for this system can be expressed as

$$\int \rho V \, d\tau = \sum_{i=1}^{N}\int_{S_i} \sigma_i V_i dS_i \quad (14)$$

where σ_i and V_i are the average surface charge density and electrostatic potential on panel *i*. Because the average potential V_i on panel *i* can also be expressed as the sum of the electrostatic potentials induced by each of the N conductor panels, (15) can be expanded as follows:

$$\int \rho V \, d\tau = \sum_{i=1}^{N}\int_{S_i} \sigma_i \left[\sum_{j=1}^{N}\int_{S_j}\frac{\sigma_j}{4\pi\varepsilon_r\varepsilon_0}\frac{1}{r_{ij}}dS_j\right]dS_i \quad (15)$$

Finally, rearranging the sums and integrals in (16) equates the volume integral of ρV with the quadratic form of the potential matrix P:

$$\begin{aligned}\int \rho V \, d\tau &= \sum_{i=1}^{N}\sum_{j=1}^{N}\frac{q_i q_j}{S_i S_j}\int_{S_i}\int_{S_j}\frac{1}{4\pi\varepsilon_r\varepsilon_0}\frac{1}{r_{ij}}dS_j dS_i \\ &= \sum_{i=1}^{N}\sum_{j=1}^{N} P_{ij} q_i q_j = \left[q^T\right]\left[P\right]\left[q\right]\end{aligned} \quad (16)$$

It follows then, that the potential matrix P for a system of N conductors is positive definite:

$$\left[q^T\right]\left[P\right]\left[q\right] > 0 \tag{17}$$

To demonstrate the positive definiteness of the sparse approximation given by (10), consider a system comprised of N conductor panels. Centered around each point on a panel, assume there exists a spherical charge distribution with radius r_0 such that the potential due to that point charge and the spherical shell combined is described by (10). There would then be N distributions of charge, "shells of image charge" for N conductor panels. The potential matrix P, whose quadratic form represents the volume integral of ρV for the entire system, can be partitioned into panel and shell contributions.

$$P = \begin{bmatrix} P_p & P_{p,sh} \\ P_{p,sh}^T & P_{sh} \end{bmatrix} \tag{18}$$

In the matrix P, P_p is the potential matrix for the N conductor panels, P_{sh} is the potential matrix for the N shells of image charge, and $P_{p,sh}$ is the matrix of coupling potentials between these two systems. Because the total, the panels, and the shells of image charges all represent "physically" realizable charge distributions, their respective matrices P, P_p, and P_{sh} are all positive definite. That is, given conductor segment currents $q_{p1}, q_{p2}, .. q_{pN}$ and shell currents $q_{sh\,1}, q_{sh\,2}, .. q_{sh\,N}$,

$$\begin{bmatrix} q_p^T & q_{sh}^T \end{bmatrix}\begin{bmatrix} P_p & P_{p,sh} \\ P_{p,sh}^T & P_{sh} \end{bmatrix}\begin{bmatrix} q_p \\ q_{sh} \end{bmatrix} > 0 \tag{19}$$

$$\left[q_p^T\right]\left[P_p\right]\left[q_p\right] > 0 \tag{20}$$

$$\left[q_{sh}^T\right]\left[P_{sh}\right]\left[q_{sh}\right] > 0 \tag{21}$$

The sparse potential matrix $\mathcal{P}$ we propose is found by using (10) as the Green's function in (5) is also given by

$$\mathcal{P} = P_p - P_{p,sh} \tag{22}$$

Hence, (20), (21), and (22) can be manipulated to show this matrix is positive definite.

When the shell charges are equal and opposite to the panel charges (i.e. q_p=q and q_{sh}=-q), (20) can be reordered and expanded as follows:

$$\left[q^T\right]\left[P_p\right]\left[q\right] - 2\left[q^T\right]\left[P_{p,sh}\right]\left[q\right] + \left[q^T\right]\left[P_{sh}\right]\left[q\right] > 0 \tag{23}$$

Because the panel charges represent a similar but denser charge distribution than the shells of equal and opposite charge, their assembly energy (given by (21) with $q_p = q$), is greater than the assembly energy of the shells of image charge (given by (22) with $q_{sh} = -q$). Therefore, (21) can be substituted into (24) without changing the inequality, and hence, the positive definiteness of the sparse matrix $\mathcal{P}$ is shown.

$$\begin{aligned} 2\left[q^T\right]\left[\mathcal{P}\right]\left[q\right] &= 2\left[q^T\right]\left[P_p - P_{p,sh}\right]\left[q\right] \geq \\ \left[q^T\right]\left[P_p\right]\left[q\right] - 2\left[q^T\right]\left[P_{p,sh}\right]\left[q\right] + \left[q^T\right]\left[P_{sh}\right]\left[q\right] &\geq 0 \end{aligned} \tag{24}$$

V. BEM Extraction with Sparse Matrices

Sparse, shift-and-truncate potential matrices can be used either directly or indirectly in BEM capacitance extraction. The direct method is procedurally identical to the conventional BEM capacitance extraction just described. A potential matrix is still obtained using a method of moments computation ((10) can be substituted into (5) if a solution by Galerkin's method is desired). Furthermore, this potential matrix P is still "inverted", and subsequently pre-multiplied by A^T and post-multiplied by A (where A is the appropriate incidence matrix) to formulate the short circuit capacitance matrix. When a ground plane is present, the procedure concludes with the formulation of two terminal capacitances. When no ground plane is present, the procedure continues on with the formulation of node pair capacitances.

When more accurate results are required for both total capacitance and individual coupling terms, either larger shift radii (and hence denser matrices) can be considered, or small radii and extremely sparse matrices can be used to precondition the dense linear problem. When a large dense linear problem is preconditioned, the sparse matrix is first inverted (i.e. factored using a direct method such as LU or Cholesky factorization), and this matrix inverse is then used to improve both the initial guess and the condition number, and hence the convergence [15], of the dense linear problem.

For example, let P and P_{st} represent the full Coulomb potential matrix and the sparse shift-and-truncate approximation. The linear problem

$$\left[P_{st}^{-1} \cdot P\right] q = P_{st}^{-1} V \tag{25}$$

will converge more rapidly than

$$Pq = V \tag{26}$$

because the condition number of ($P_{st}^{-1} \cdot P$) is smaller than that of P. The sparse partial inductance matrices described in [9] have been similarly applied to precondition the multipole-iterative circuit reductions employed in FastHenry [8].

VI. Examples

The direct use of shift-and-truncate matrices in BEM capacitance extraction (relative to truncation only and full matrix formulations) was tested in terms of a simple extraction program. The potential matrix P was formulated using a discrete implementation of the Galerkin method (which produces a symmetric matrix). Because P can be a very large, albeit a sparse matrix when shift-and-truncation or truncation formulations are used, (7) was solved iteratively using the Conjugate Gradient Method (CGM) [7].

Consider the interconnect wiring example depicted in Fig.5. Twenty-one wires on three wiring levels are embedded in a dielectric ε_1 of thickness h_d which is in turn, sandwiched between an ideal ground plane below and the air above. The

seven parallel wires on the first wiring plane (the wiring plane closest to the ground plane) are orthogonally crossed by seven parallel wires on the second wiring plane, which in turn, are orthogonally crossed by seven parallel wires on the third wiring plane. Wire thicknesses, wire widths and pitches, and interlevel spacings are 0.5, 0.5, 1.5, and 0.5 microns respectively. Separation between the ideal ground plane and the first wiring layer is h_{gp}, and the dielectric layer ε_1 has a relative dielectric constant of four. The twenty-one conductors were uniformly subdivided into 0.5 μm x 0.5 μm panels. (This discretization produces a fully dense 1638x1638 matrix when the full Coulomb potentials are considered.)

To demonstrate the feasibility of using the sparse image (or shift-and-truncate) method directly we computed total line capacitance (the diagonal term in the C_{ss} matrix) for each of the twenty one lines in Fig.5 using three formulations of the electrostatic potential matrix (the full matrix, a shift-and-truncate matrix, and an equally sparse truncated matrix) and three combinations of h_{gp} and h_d ([∞, ∞], [0.5μm, ∞], and [0.5μm, 3.5μm]). When shift and truncate potentials were considered, the shift radius r_0 in (10) was set to 2.4 μm (which in turn made the potential matrices 88.8% sparse). When truncated potentials were considered, an unshifted ($r_0 = \infty$) but truncated matrix of equal sparsity was considered. In every case, CGM iterations were continued until the Euclidean norm of the residual ($\|Ax-b\|_2$) was less than 10^{-3}.

Consider the results listed in Table 1 for the case of an infinite dielectric without a ground plane ($h_{gp} = \infty$ and $h_d = \infty$). The sparse image method provided reasonably accurate estimates of total line capacitance for this example (within 6% of the full matrix results for all lines except 1, 7, 15, and 21—which are outlying lines with unrealistic boundaries—where the error approached 14%). On the other hand, BEM capacitance extraction using an equally sparse, truncated matrix erred by as much as 41%.

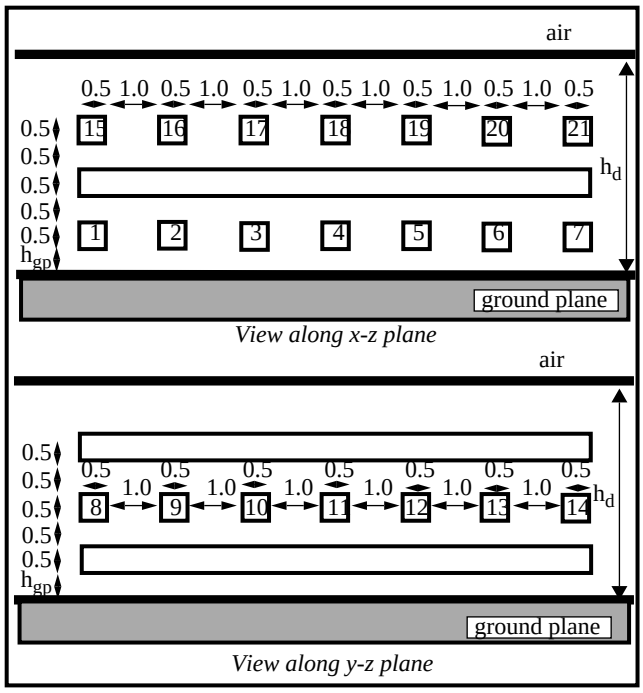

FIGURE 5: Seven wire busses with three wiring levels and ground plane.

TABLE 1. Total Capacitance in fempto-Farads for 21 Conductors in Fig.5 with $h_{gp} = \infty$ and $h_d = \infty$.

	Coulomb Potentials	**Shift and Truncate**	**Truncation Only**
C_1, C_7	1.318	1.499	1.534
C_2, C_6	1.490	1.572	1.950
C_3, C_5	1.492	1.573	2.099
C_4	1.492	1.573	2.136
C_8, C_{14}	1.603	1.679	1.807
C_9, C_{13}	1.765	1.779	2.228
C_{10}, C_{12}	1.766	1.780	2.439
C_{11}	1.766	1.780	2.497
C_{15}, C_{21}	1.318	1.499	1.534
C_{16}, C_{20}	1.490	1.572	1.950
C_{17}, C_{19}	1.492	1.573	2.099
C_{18}	1.492	1.573	2.136

While it's almost impossible to interpret the source of the error in the truncated results (remember, simply discarding the smallest elements in a potential matrix can render these matrices indefinite), the source of error in the shift and truncate case is obvious. Lines 1, 7, 15, and 21 lack near neighbor coupling on two of their four sides. The shift-and-truncate formulation, because it assumes a minimum coupling distance, over predicts total capacitance for these lines. But if the shift radius is r_0 increased, even the accuracy of these predictions will improve to acceptable levels.

Besides improved accuracy, the shift and truncate extraction also converges faster. For this first example, the shift and truncate extraction converged in 381 CGM iterations, while the full and truncated matrix extractions required 473 and 2546 CGM iterations respectively.

Next, consider the results listed in Table 2 for the case of an infinite dielectric over a ground plane ($h_{gp} = 0.5$ μm and $h_d = \infty$). BEM capacitance extraction using shift-and-truncate potentials again provided very accurate estimates of total line capacitance (within 5% of the Coulomb potential results for all lines except the lightly coupled outside lines 15 and 21). BEM capacitance extraction using truncated Coulomb potentials, however, also produced accurate results (within 8% of the full matrix results).

This improvement is due to the presence of a ground plane. The discarded terms in the truncated matrix now represent dipole rather than monopole terms (see the equation in Fig.2), and hence, second order effects. The truncated extraction, however, was still more costly to compute than the shift-and-truncate extraction. The shift-and-truncate extraction converged in 382 iterations, while the full and truncated extractions required 428 and 513 iterations respectively.

Finally, consider the results listed in Table 2 for the case of a thin dielectric layer over a ground plane ($h_{gp} = 0.5$ μm and $h_d = 3.5$ μm). Again, the sparse image method provided accu-

TABLE 2. Total Capacitance in fempto-Farads for 21 Conductors in Fig.5 with h_{gp} = 0.5 μm and $h_d = \infty$.

	Coulomb Potentials	Shift and Truncate	Truncation Only
C_1, C_7	1.789	1.777	1.814
C_2, C_6	1.857	1.853	1.891
C_3, C_5	1.857	1.854	1.895
C_4	1.857	1.854	1.895
C_8, C_{14}	1.627	1.691	1.671
C_9, C_{13}	1.766	1.792	1.835
C_{10}, C_{12}	1.766	1.793	1.852
C_{11}	1.766	1.793	1.853
C_{15}, C_{21}	1.334	1.500	1.403
C_{16}, C_{20}	1.492	1.572	1.592
C_{17},C_{19}	1.493	1.573	1.614
C_{18}	1.493	1.573	1.616

rate estimates of the total line capacitance (within 5% of the Coulomb potential results for all lines except the lightly coupled outside lines 15 and 21), and converged in fewer iterations than either the full and truncated extractions (387 versus 434 and 596 CGM iterations respectively). Furthermore, because the shift-and-truncate formulation provides a natural and consistent truncation scheme for the infinite series in (12), the potential matrix was also easier to formulate.

VII. Conclusions

The shift-and-truncate approximation proposed in [9] for partial inductance extraction has been successfully applied to BEM capacitance extraction for uniform and multilayered planar dielectrics. Because it naturally truncates the method of images solution, this sparse image method yields both a sparse and an easily-formulated potential matrix for the multilayered dielectric case (which is generally problematic because of the complex Green's functions that arise). Total line capacitance was obtained for practical examples using both full and sparse matrix formulations. Because the sparse image method proposed yielded a better conditioned matrix than simple truncation, the iterative method employed in these examples was also shown to converge faster for shift-and-truncate matrices.

TABLE 3. Total Capacitance in fempto-Farads for 21 Conductors in Fig.5 with h_{gp} = 0.5 μm and h_d = 3.5 μm

	Coulomb Potentials	Shift and Truncate	Truncation Only
C_1, C_7	1.788	1.777	1.821
C_2, C_6	1.858	1.852	1.903
C_3, C_5	1.858	1.853	1.908
C_4	1.858	1.853	1.908
C_8, C_{14}	1.621	1.686	1.679
C_9, C_{13}	1.766	1.786	1.862
C_{10}, C_{12}	1.766	1.788	1.890
C_{11}	1.766	1.788	1.893
C_{15}, C_{21}	1.220	1.387	1.298
C_{16}, C_{20}	1.393	1.458	1.539
C_{17},C_{19}	1.393	1.459	1.578
C_{18}	1.393	1.459	1.584

References

[1] T.M.Apostol, *Mathematical Analysis, A Modern Approach to Advanced Calculus*, Addison-Wesley, Reading Mass., 1957.

[2] C.A. Brebbia, *Boundary Element Method for Engineers*, Pentech Press, London, 1978.

[3] U.Choudhury and A.Sangiovanni-Vincentelli, "Automatic Generation of Analytical Models for Interconnect Capacitances", *IEEE Transactions on Computer-Aided Design*, 14, No. 5, April 1995.

[4] R.F.Harrington, *Field Computation by Moment Methods*, Macmillan, New York, 1968.

[5] H.A.Haus and J.R.Melcher, *Electromagnetic Fields and Energy*, Prentice Hall, Englewood Cliffs, New Jersey, 1989.

[6] T.F.Hayes and J.J.Barrett, "Modeling of Multiconductor Systems for Packaging and Interconnecting High-Speed Digital IC's", *IEEE Transactions on Computer-Aided Design*, 11, No. 4, April 1992.

[7] M.R.Hestenes and E.Stiefel, "Methods of Conjugate Gradients for Solving Linear Systems", Journal of Research of the National Bureau of Standards, Vol. 49, No. 6, Dec. 1952.

[8] M.Kamon, B.Krauter, J.Phillips, L.T.Pileggi, and J.White, "Two Optimizations to Accelerated Method-of-Moments Algorithms for Signal Integrity Analysis of Complicated 3-D Packages", *Proc. of the IEEE 4th Topical Meeting on Electrical Performance of Electronic Packaging*, Oct. 1995.

[9] B.Krauter and L.T.Pileggi, "Generating Sparse Partial Inductance Matrices with Guaranteed Stability", *IEEE/ACM Intl. Conf. on Computer Aided Design*, Nov. 1995.

[10] D.D.Ling and A.E.Ruehli, "Interconnection Modeling: Lumped Circuit Element Models," *Circuit Analysis, Simulation and Design, Advances in CAD for VLSI Vol. 3, Part II*, Edited by A.E.Ruehli, Slivers Science Publishers B.V., Mastered, 1987.

[11] P.Lorrain and D. Corson, *Electromagnetic Fields and Waves*, 2nd Edition, W.H.Freeman and Company, San Francisco, 1970.

[12] K.Nabors and J.K.White, "FASTCAP: A Multipole Accelerated 3-D Capacitance Extraction Program", *IEEE Transactions on Computer-Aided Design*, 10, No. 11, Nov. 1991.

[13] P.D.Patel, "Calculation of Capacitance Coefficients for a System of Irregular Finite Conductors on a Dielectric Sheet", *IEEE Transactions on Microwave Theory and Techniques*, 19, No. 11, Nov. 1971.

[14] L.T.Pileggi, "Coping with RC(L) Interconnect Headaches", *IEEE/ACM Intl. Conf. on Computer Aided Design*, Nov. 1995

[15] W.Press, B.Flannery, S.Teukolsky, and W.Vetterling, *Numerical Recipes in C*, Cambridge: Cambridge University Press, 1988.

[16] A.E.Ruehli and P.A.Brennan, "Efficient Capacitance Calculations for Three Dimensional Multiconductor Systems", *IEEE Transactions on Microwave Theory and Techniques*, 21, No. 2, Feb. 1973.

[17] E.Weber, *Electromagnetic Fields, Volume I-Mapping of Fields*, John Wiley & Sons, Inc., New York, 1950.